LARGE-EDDY SIMULATION OF INTERNAL WAVE MOTIONS

DAVID A. SIEGEL

Computational Oceanography Group, Department of Geography
University of California at Santa Barbara, Santa Barbara, California, 93106

ABSTRACT

Large-eddy simulation (LES) techniques are used to numerically investigate the motions and mixing processes of the oceanic internal wave field. LES's solve the three-dimensional, nonlinear, time dependent Navier-Stokes equations for the resolved scales of motion while parameterizing the effects of the unresolved subgrid scales. This allows oceanographically relevant length and time scales to be numerically simulated using present-day supercomputers.

Here, the results (some preliminary) of two recent LES experiments of stably-stratified ocean turbulence are presented. The first experiment is the study of the decay of stably-stratified turbulence at oceanographically relevant length and time scales. The initial wavenumber distribution is consistent with the Garrett-Munk (GM) internal wave spectrum extrapolated to scales smaller than 10 m. This experiment clearly shows many features of the so-called "turbulent collapse" (i.e., the transition from a fully turbulent flow to an internal wave dominated field). However, the present results illustrate several important differences from previous laboratory and *direct* numerical results. In particular, highly anisotropic, "pancake" structures are not formed coincident with the onset of the turbulent collapse. We hypothesize that the lack of two-dimensionalization of the kinetic energy structures is due to the relatively large Reynolds numbers of the LES experiments and suggest that the results of laboratory and *direct* numerical experiments be cautiously applied to the internal wave field.

The second experiment is a preliminary attempt to use LES techniques to directly determine values of vertical eddy diffusivities for steady thermocline motions. The Navier-Stokes equations are forced to maintain constant energy, consistent with GM amplitudes, for the lowest resolved wave modes (50 m). The phases of the forced wave mode are determined dynamically by solving the equations of motion. The long time integration (≥30 Nt) and steady forcing enables the domain averaged buoyancy flux and hence, the vertical eddy diffusivity (K_{BF}) to be determined directly. Values of K_{BF} are consistent with oceanographic inferences ($6x10^{-6}$ to $6x10^{-4}$ m^2 s^{-1}) although their dependency upon the buoyancy frequency is quite anomalous (going as N^{+2}!!). This anomalous dependency is thought to be caused by the nature of the numerical forcing. The direct determinations of K_{BF} are compared with several indirect turbulent variance dissipation rate estimates. The forced LES experimental results are preliminary as many detailed analyses still need to be performed.

MODELING THE OCEANIC INTERNAL WAVE FIELD

A variety of scientific questions may be addressed using "data" obtained from the numerical simulation of the ocean's internal wave field. For instance, important parameters that are very difficult to directly measure *in situ*, such as diapycnal and isopycnal eddy diffusivities, may be directly

determined numerically. This would enable parametric dependencies to be directly investigated. Diapycnal eddy diffusivities for active (temperature and salinity) and passive (tracer) scalars may be compared to examine the importance of buoyancy on the mixing of scalars. Similarly, the parametric dependence of turbulent variance dissipation rates can be evaluated. In addition, the consistency of the linear internal gravity wave dispersion relation with the simulated "data" may be evaluated. Knowing the spatial structure and temporal evolution of the internal wave field, the potential of many oceanographic applications may be evaluated. For example, the effects of internal wave motions upon the transmission of acoustic signals can be determined using simulated "data" (e.g., T. Ewart, this volume). The sampling characteristics of oceanographic instrumentation may also be evaluated (e.g., Ledwell and Watson, 1991; Siegel and Plueddemann, 1991).

The point is that all of the above scientific questions and technical needs require "data" from the internal wave field that are difficult to obtain from current observational techniques. Here, we illustrate the application of large-eddy simulation (LES) techniques to the oceanic internal wave field as a method for *supplementing* our present observational tool set. The idea is to use *in situ* observations of the internal wave field to drive a LES model in order to calculate those properties which are difficult to obtain observationally (such as, eddy diffusivities or dissipation rates). This approach has proven to be quite successful in studies of the atmospheric boundary layer (e.g., Deardorff, 1973; Wyngaard, 1984; Ebert *et al.*, 1989).

In order to realistically simulate the internal wave field, several rather stringent requirements must be satisfied. First, it is anticipated that the motions of the internal wave field are fully three-dimensional and must be modeled that way. Second, characteristic nondimensional numbers (cf., Reynolds, Froude and Rossby) are important and must be correctly considered in any investigation. Third, relevant spatial scales range from 10's of cm's to many 100 m's, while temporal scales range from minutes to days (e.g., Garrett and Munk, 1972; 1975; Munk, 1981; Gargett *et al.*, 1981; 1984). Fourth, the internal wave field is comprised not only of *linear* internal waves, but also many turbulent and vortical motions (e.g., Holloway, 1983; Müller *et al.*, 1986; Müller, 1988). Thus, the full suite of allowable motions must be included. The most straightforward way to insure that these requirements are met is to directly solve the Navier-Stokes equations for the proper time and space scales.

Unfortunately, computational resources are finite. Only a limited number of spatial modes can be numerically simulated using present-day supercomputers (O(100) in each direction). This puts rather severe restrictions on the spatial domain that one can investigate by *directly* solving the Navier-Stokes equations. When directly solving the Navier-Stokes equations, *all* scales relevant to the transport and dissipation of energy *must* be explicitly resolved. The bandwidth of required spatial scales is described by the Reynolds number (e.g., Tennekes and Lumley, 1972). For the oceanic internal wave field, Reynolds numbers ($u'h/\nu$; where ν is the kinematic viscosity = 10^{-6} m^2 s^{-1}) based upon a 1 m overturning length scale (h) and a velocity scale (u') of 0.1 m s^{-1} are O(10^5). This indicates that molecular processes are not directly relevant to the internal wave field's evolution. Values of the Reynolds number (Re_λ) based upon the Taylor length scale ($\lambda=u'/(\partial u/\partial x)'$ for an isotropic field) are often used for comparing dissimilar approaches of studying turbulence (e.g., Lesieur, 1987). For the oceanic internal wave field, values of Re_λ are O(10^5) (using u'=0.1 m s^{-1} and $\varepsilon_{KE}=10^{-8}$ m^2 s^{-3}). However for laboratory and *direct* numerical simulations of stably-stratified turbulence, reported

values of Re_λ are always less than 100 (e.g., Riley *et al.*, 1981; Stillinger *et al.*, 1983; Itsweire *et al.*, 1986; Holloway and Ramsden, 1988; Métais and Herring, 1989; Lienhard and Van Atta, 1990; Ramsden and Holloway, 1991). Thus, it is clear that both laboratory and *direct* numerical investigations can not adequately simulate the oceanic internal wave field. This is not to say that these experiments have not given valuable insights into the innerworkings of stably-stratified turbulence, just that they cannot realistically simulate the ocean's internal gravity wave field.

SIMULATING THE LARGE EDDIES

To get around the finite resolution afforded by present computational resources, we apply the large-eddy approximation (e.g., Deardorff, 1970; 1973; Schumann, 1975; Ferziger, 1983; Wyngaard, 1984; Rogallo and Moin, 1984; Lesieur, 1987). In a large-eddy simulation (LES), the large, or grid scale (GS), motions are directly simulated while the effects of the subgrid scales (SGS) are parameterized in terms of the GS. Most importantly, the modeling of the SGS processes allows oceanographically relevant Reynolds numbers to be simulated in a numerically achievable wavespace. The application of the large-eddy approximation means that the GS motions contain the energy of the flow and perform the mixing (that is, support a buoyancy flux), while the SGS eddies act to dissipate energy as part of the turbulent cascade. This separation of the dynamical roles of the GS and SGS motions provides a useful means of examining the consistency of a LES. That is, GS energy levels should be much greater than the SGS, while the GS dissipation rates must be much smaller than the SGS rates of dissipation. These simple concepts are helpful for evaluating LES model performance.

In a LES, the cutoff scale between GS and SGS motions is generally made within the inertial subrange of turbulence. This is done for two reasons. First, motions at these spatial scales should be locally isotropic. Second, the rate at which kinetic (KE) and potential (PE) energies are transferred across the SGS cutoff must be equal to the rate at which they are dissipated by molecular processes (the KE and PE dissipation rates, ϵ_{KE} and ϵ_{PE}). These facts make the parameterization of SGS processes simpler than second moment turbulence closures which must hold over all scales of motion.

It is important to recognize that the essential difference between a large-eddy simulation and a *direct* simulation of any turbulent flow is the development of a parameterization for the effects of the SGS processes in terms of the resolved scale dynamics. In some sense, the degree that the large-eddy simulation conforms to its intended reality is a function of how well the SGS parameterization performs its task. This suggests that one must carefully choose a SGS parameterization method. Unfortunately, there have been very few comparison studies of SGS model performance (e.g., Clark *et al.*, 1979; Schumann, 1991). However, these results, as well as some reported here, indicate that the choice of SGS models makes little difference to the resolved scale energetics. This result is not really unexpected as the GS cutoff is made within the inertial subrange of turbulence and the SGS motions have "forgotten" the orientation of the GS motions that are driving them. This means that a simple statistical accounting of the GS energy sink due to SGS energy cascade, such as by a uniform eddy viscosity, may be enough to successfully simulate the large scale motions (e.g., Lesieur, 1987).

LES techniques have long been applied to atmospheric science and engineering problems (e.g., Deardorff, 1970; 1973; 1980; Schumann, 1975; 1991; Ferziger, 1983; Wyngaard, 1984; Rogallo and Moin, 1984; Moeng, 1984; Eidson, 1985; Lesieur, 1987; Moeng and Wyngaard, 1988; Schmidt and

Schumann, 1989; Mason and Derbyshire, 1990). However, they have only been recently applied to oceanographic flows (e.g., Siegel, 1988; 1991; Gallacher, 1990; McWilliams *et al.*, 1990; Siegel and Domaradzki, 1991a; 1991b). One should note that the modeling of SGS processes is similar in spirit to the parameterization of SGS processes in eddy-resolving oceanic general circulation models (e.g., Holland and Lin, 1975). The major difference is that more is known about the dynamics of 3-D, locally isotropic turbulence than about submesoscale (O(1-10 km)) ocean motions.

Here, we will illustrate the development of a LES model and its application for investigating the interactions among internal gravity waves and turbulence within the thermocline. One of our goals is to use LES techniques as a predictive tool for evaluating the magnitude and parametric dependence of diapycnal and isopycnal eddy diffusivities for use in regional and global scale ocean circulation models. Here, we will describe the results of two LES experiments. The first experiment describes the decay of stably-stratified turbulence at oceanic space and time scales, while the second applies a LES model to directly determine values of the diapycnal eddy diffusivity. This work is preliminary, but clearly illustrates a "proof of concept".

DEVELOPMENT OF A LES MODEL FOR THE INTERNAL WAVE FIELD

The motions of the resolved scale eddies are determined by solving the 3-D Navier-Stokes equations for an incompressible fluid, satisfying the Boussinesq approximation, where temperature is the active scalar. Using these assumptions, the equations of motion are

$$\frac{\partial u_i}{\partial t} = -\frac{\partial u_i u_j}{\partial x_j} - \frac{\partial p}{\partial x_i} + a g d_{i3} T + n \frac{\partial^2 u_i}{\partial x_j \partial x_j} + F_i \tag{1a}$$

$$\frac{\partial T}{\partial t} = -\frac{\partial T u_j}{\partial x_j} - u_3 \frac{dT_s}{dx_3} + k \frac{\partial^2 T}{\partial x_j \partial x_j} + F_T \tag{1b}$$

$$\frac{\partial u_i}{\partial x_i} = 0 \tag{1c}$$

where t is time, x_i is the spatial vector (x; x_1,x_2,x_3; x,y,z), u_i is the velocity vector (u; u_1,u_2,u_3; u,v,w), p is the pressure perturbation from the hydrostatic balance (normalized by the mean density), T is the perturbation temperature from the horizontal mean temperature ($T_s(x_3)$), which describes the stable background profile), g is the magnitude of the vertical gravitational acceleration (9.8 m s^{-2}), a is the coefficient of thermal expansion (0.025 K^{-1}), n is the kinematic viscosity (10^{-6} m^2 s^{-1}), and k is the thermal conductivity (10^{-6} m^2 s^{-1}), d_{i3} is the Kronecker-delta function and F_i and F_T represent external forcing functions. The degree of stable stratification is characterized by the buoyancy frequency, N, which is equal to

$$N = \left(\alpha g \, \delta_{i3} \frac{dT_s}{dx_i} \right)^{1/2} \tag{2}$$

The domain is a triply-periodic cube with sides of length, L. The boundary conditions are

$$u_i(x_j) = u_i(x_j + nL) \tag{3a}$$

$$T(x_j) = T(x_j + nL) \tag{3b}$$

where n is any integer. This allows spectral numerical techniques to be applied, enabling the spatial terms to be expanded using Fourier series (Orszag, 1971). Periodic boundary conditions are appropriate for the numerical simulation of statistically homogeneous flows (Lesieur, 1987).

The equations of motion are nondimensionalized using the box size, $L/2\pi$, as the length scale, the buoyancy period, N^{-1}, as the time scale, and α^{-1} as the temperature scale. The factor of 2π in the definition of the length scale enables spatial wavenumbers to be defined as integer values. Hereafter, the nondimensionalized forms of the equations of motion will be utilized.

In developing a LES model, the equations of motion are *volume* averaged to define the grid scale motions distinct from the SGS. This filtering operation partitions a fluid variable ($f(\mathbf{x};t)$) into GS ($\bar{f}(\mathbf{x};t)$) and SGS ($f'(\mathbf{x};t)$) components (Leonard, 1974),

$$f(\mathbf{x};t) = \bar{f}(\mathbf{x};t) + f'(\mathbf{x};t) \tag{4}$$

The GS value of $f(\mathbf{x};t)$ is evaluated as its convolution with a spatial filtering function ($G(\mathbf{x})$), or

$$\bar{f}(\mathbf{x};t) = \int_D G(\mathbf{x}-\mathbf{x}')\, f(\mathbf{x}';t)\, d\mathbf{x}' \tag{5}$$

where the integration is taken over the entire domain, D. A boxcar average in physical space is often used for $G(\mathbf{x})$, or

$$G(\mathbf{x}) = \begin{cases} 1 & |\mathbf{x}| < \Delta \\ 0 & |\mathbf{x}| > \Delta \end{cases} \tag{6}$$

where Δ is the physical space grid-scale ($\Delta=L/N_x$; where N_x is the numerical resolution in the x-direction). This boxcar averaging procedure is implicit in the pioneering large-eddy simulations of Deardorff (1970) and Schumann (1975) and is appropriate when the SGS fluxes and stresses are parameterized in physical space. There are many other filtering operators that may be applied in physical space (e.g., Leonard, 1974; Ferziger, 1983). Alternatively, the filtering may be preformed in spectral space, following

$$\bar{f}(\mathbf{k};t) = \int_D G(\mathbf{k}-\mathbf{k}')\, f(\mathbf{k}';t)\, d\mathbf{k}' \tag{7}$$

where $\mathbf{k}$ is the vector wavenumber (k_i; k_1,k_2,k_3) and $G(\mathbf{k})$ is the spectral filtering function which is often a sharp-cut filter ($G(\mathbf{k})=1$ if $|\mathbf{k}|<k_c$; $G(\mathbf{k})=0$, elsewhere; where k_c is the GS cutoff wavenumber=π/Δ). Spectral filtering is appropriate when the SGS parameterization is made in spectral space. Gaussian filtering functions (which are the same in spectral and physical space) may also be used for $G(x)$ (e.g., Mansour *et al.*, 1979; Ferziger, 1983; Piomelli *et al.*, 1989). For the present application, the advantages of these procedures do not appear to outweigh the cost, complexity and possible ambiguities in the interpretation of the resulting simulations (Clark *et al.*, 1979; Ferziger, 1983; Eidson, 1985). However, this may not be true for inhomogeneous flows, such as wall-bounded flows (Ferziger, 1983; Piomelli *et al.*, 1989).

Application of either of the averaging procedures (eqns. 5 or 7) to the nondimensionalized equations of motion gives

$$\frac{\partial \bar{u}_i}{\partial t} = -\frac{\partial \overline{u_i u_j}}{\partial x_j} - \frac{\partial \bar{p}}{\partial x_i} + g\delta_{i3}\bar{T} + \nu \frac{\partial^2 \bar{u}_i}{\partial x_j \partial x_j} + \bar{F}_i \tag{8a}$$

$$\frac{\partial \bar{T}}{\partial t} = -\frac{\partial \overline{u_j T}}{\partial x_j} - \bar{u}_3 \frac{dT_s}{dx_3} + \kappa \frac{\partial^2 \bar{T}}{\partial x_j \partial x_j} + \bar{F}_T \tag{8b}$$

$$\frac{\partial \bar{u}_i}{\partial x_i} = 0 \tag{8c}$$

where the summation convention is used. The nonlinear flux terms also need to be partitioned into GS and SGS components.

$$\overline{u_i u_j} = \overline{\bar{u}_i \bar{u}_j} + \overline{u'_i \bar{u}_j} + \overline{\bar{u}_i u'_j} + \overline{u'_i u'_j} = \bar{u}_i \bar{u}_j + \Lambda_{ij} - \tau_{ij} \tag{9a}$$

$$\overline{u_i T} = \overline{\bar{u}_i \bar{T}} + \overline{u'_i \bar{T}} + \overline{\bar{u}_i T'} + \overline{u'_i T'} = \bar{u}_i \bar{T} + \Lambda_{\theta i} - \tau_{\theta i} \tag{9b}$$

where Λ_{ij} is the Leonard momentum flux ($\overline{\bar{u}_i \bar{u}_j} - \bar{u}_i \bar{u}_j$), $\Lambda_{\theta i}$ is the Leonard heat flux ($\overline{\bar{u}_i \bar{T}} - \bar{u}_i \bar{T}$), τ_{ij} is the SGS momentum flux ($\overline{u'_i u'_j} + \overline{u'_i \bar{u}_j} + \overline{\bar{u}_i u'_j}$), and $\tau_{\theta i}$ is the SGS heat flux ($\overline{u'_i T'} + \overline{u'_i \bar{T}} + \overline{\bar{u}_i T'}$). The Leonard fluxes are a consequence of the nested averaging procedure (Leonard, 1974) and will be neglected presently. Leonard fluxes are identically zero when a sharp-cut spectral filter is used and are very small when boxcar averaging in physical space is applied (e.g., Leonard, 1974; Clark *et al.*, 1979; Yoshizawa, 1982; Ferziger, 1983; Eidson, 1985). However, the Leonard fluxes must be considered when a Gaussian filter is used.

Applying the above definitions of the SGS fluxes and writing the GS nonlinear terms in the momentum equation in vorticity form (to insure numerical stability), the GS equations of motion may be expressed as

$$\frac{\partial \bar{u}_i}{\partial t} = \varepsilon_{ijk} \bar{u}_j \bar{\Omega}_k - \frac{\partial \bar{p}}{\partial x_i} - \frac{\partial (\bar{u}_j \bar{u}_j)/2}{\partial x_i} + g \delta_{i3} \bar{T} + \nu \frac{\partial^2 \bar{u}_i}{\partial x_j \partial x_j} - \frac{\partial \tau_{ij}}{\partial x_j} + \bar{F}_i \tag{10a}$$

$$\frac{\partial \bar{T}}{\partial t} = -\frac{\partial \bar{u}_j \bar{T}}{\partial x_j} - \bar{u}_3 \frac{dT_s}{dx_3} + \kappa \frac{\partial^2 \bar{T}}{\partial x_j \partial x_j} - \frac{\partial \tau_{\theta j}}{\partial x_j} + \bar{F}_T \tag{10b}$$

$$\frac{\partial \bar{u}_i}{\partial x_i} = 0 \tag{10c}$$

where $\bar{\Omega}_i$ is the GS vorticity vector ($\bar{\Omega}_i = \varepsilon_{ijk} \partial \bar{u}_k / \partial x_j$) and ε_{ijk} is the alternating tensor. These equations are then solved, for specific forcing conditions, to give the evolution of the GS velocity and temperature fields. First the SGS momentum and heat fluxes (τ_{ij} and $\tau_{\theta j}$) need to be parameterized in terms of the GS velocity and temperature fields.

SUBGRID SCALE PARAMETERIZATION METHODOLOGIES

Many different methodologies have been employed for parameterizing SGS fluxes in LES models. SGS parameterizations that are applied in physical space range from very simple "production equals dissipation" SGS energy budget approaches (e.g., Smagorinsky, 1963; 1990; Clark *et al.*, 1979; Eidson, 1985; Mason and Derbyshire, 1990; Siegel and Domaradzki, 1991a) to detailed evaluations of the entire SGS energy budget (e.g., Deardorff, 1980; Moeng, 1984; Schmidt and Schumann, 1989; Gallacher, 1990). On the other hand, spectral SGS parameterizations have been developed based upon turbulence closure theory calculations of the rate of energy transfer across the GS cutoff and are

usually applied in wavenumber space (e.g., Kraichnan, 1976; Chollet and Lesieur, 1981; Lesieur, 1987; Domaradzki *et al.*, 1987; Yakhot *et al.*, 1989). Unfortunately, detailed intercomparison studies of these SGS parameterization methods are lacking for stably-stratified turbulent flows (see Schumann, 1991 for a recent exception).

Here, we discuss and apply two different SGS parameterization methods, the physically-based Smagorinsky SGS eddy viscosity and the spectral Chollet and Lesieur (1981; hereafter CL81) eddy viscosity. Preliminary comparisons that we have made indicate that the evolution of the GS energetics is essentially the same for the two different SGS eddy viscosities. However, the GS energy spectra produced using the CL81 spectral eddy viscosity reflect spectral levels and slopes closer to theoretical Kolmogorov "5/3" spectra than do those produced using the Smagorinsky eddy viscosity (fig. 1). Before our LES results are discussed, it is important to address how SGS parameterizations are made.

The SGS fluxes and stresses are most often represented in flux-gradient form, or

$$\tau_{ij} = - K_{SGS} \bar{S}_{ij} + \frac{\tau_{kk}}{3} \delta_{ij} \tag{11a}$$

$$\tau_{\theta i} = - \frac{K_{SGS}}{Pr_t} \frac{\partial \bar{T}}{\partial x_i} \tag{11b}$$

where K_{SGS} is the SGS eddy viscosity (a function of x and t), $\bar{S}_{ij}$ is the GS rate of strain tensor $(\partial \bar{u}_i/\partial x_j + \partial \bar{u}_j/\partial x_i)$, and Pr_t is the SGS turbulent Prandtl number (the ratio of the SGS eddy viscosity to the SGS eddy diffusivity). The final equations of motion are

$$\frac{\partial \bar{u}_i}{\partial t} = \varepsilon_{ijk} \bar{u}_j \bar{\Omega}_k - \frac{\partial \bar{\pi}}{\partial x_i} + g \delta_{i3} \bar{T} + \nu \frac{\partial^2 \bar{u}_i}{\partial x_j \partial x_j} + \frac{\partial}{\partial x_j}\left(K_{SGS} \bar{S}_{ij}\right) + \bar{F}_i \tag{12a}$$

$$\frac{\partial \bar{T}}{\partial t} = - \frac{\partial \bar{u}_j \bar{T}}{\partial x_j} - \bar{u}_3 \frac{dT_s}{dx_3} + \kappa \frac{\partial^2 \bar{T}}{\partial x_j \partial x_j} + \frac{\partial}{\partial x_j}\left(\frac{K_{SGS}}{Pr_t} \frac{\partial \bar{T}}{\partial x_j}\right) + \bar{F}_T \tag{12b}$$

$$\frac{\partial \bar{u}_j}{\partial x_j} = 0 \tag{12c}$$

where $\bar{\pi}$ is the pressure head which includes the GS $(\bar{u}_k \bar{u}_k/2)$ and SGS $(\tau_{kk}/3)$ normal stresses.

Once the SGS eddy viscosity and forcing functions are specified, this system of equations can be solved directly for the evolution of the GS flow. We employ pseudo-spectral numerical techniques, based upon Fourier series expansions, to solve for the spatial terms of the equation of motion and advance time using the leap-frog method (e.g., Orszag, 1971; Siegel, 1988; Canuto *et al.*, 1988). These methods are highly accurate and are standard in numerical turbulence investigations. A complete description of the numerical methods used may be found in Siegel (1988).

THE SMAGORINSKY SGS EDDY VISCOSITY

The Smagorinsky SGS eddy viscosity is derived assuming that K_{SGS} depends only upon the smallest resolvable scale (Δ) and the rate at which KE is transferred across the GS cutoff (Δ). For the inertial subrange of turbulence, the spectral transfer of KE is equal to the KE dissipation rate, ε_{KE}. Applying only dimensional arguments, K_{SGS} is given by

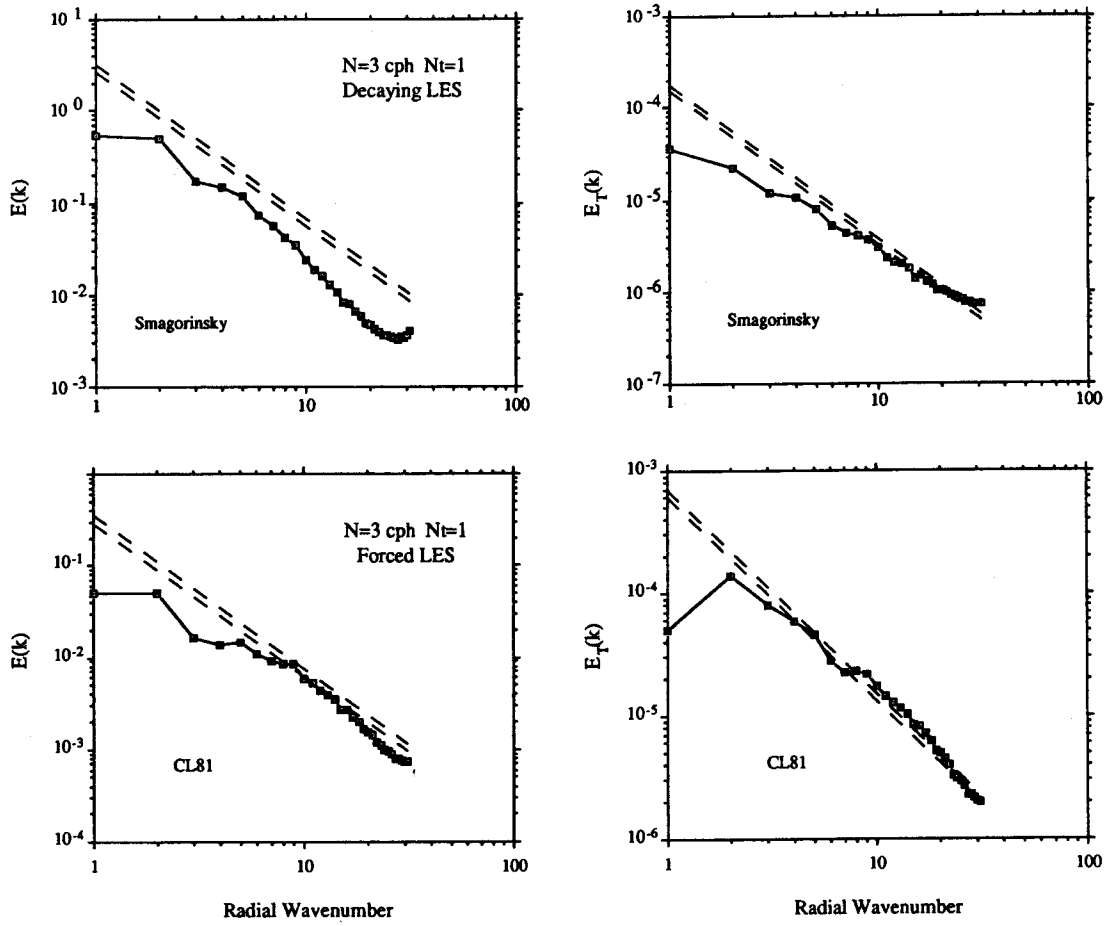

Figure 1: Comparison of radial wavenumber kinetic energy and temperature variance spectra calculated using the Smagorinsky SGS eddy viscosity (upper) and the CL81 eddy viscosity (lower). The dotted lines are theoretical inertial subrange Kolmogorov spectra for KE ($E(k) = \alpha_K \varepsilon^{2/3} k^{-5/3}$) and for temperature variance ($E_T(k) = \beta_K \chi \varepsilon^{-1/3} k^{-5/3}$, where χ is the temperature variance dissipation rate). The two lines express the magnitude of experimental uncertainty in the values of the Kolmogorov constants, α_K and β_K.

$$K_{SGS} = (c_s \Delta)^{4/3} \varepsilon_{KE}^{1/3} \tag{13}$$

where the constant of proportionality (c_s) is referred to as the Smagorinsky constant. To evaluate the value of K_{SGS} at any point in space, the energy transfer rate (ε_{KE}) must be known at that location. In general, ε_{KE} depends on all scales of motion. However, the SGS fluxes must be parameterized in terms of the GS motions alone. For a statistically homogeneous flow, such within the turbulent inertial subrange, the dissipation of KE is equal to its production, or

$$\varepsilon_{KE} = -\frac{1}{2} \bar{S}_{ij} \tau_{ij} + g \delta_{i3} \tau_{\theta i} \tag{14}$$

Here, the dissipation of KE is balanced by the turbulent production by the GS shear ($\bar{S}_{ij}$) and by the

SGS buoyancy flux ($g\,\delta_{i3}\,\tau_{\theta i}$). Applying the flux-gradient forms of the SGS fluxes (eq. 11) results in

$$\varepsilon_{KE} = \frac{1}{2} K_{SGS}\,\bar{S}^2 - \frac{g}{Pr_t} K_{SGS} \frac{\partial \bar{T}}{\partial x_3} \tag{15}$$

where $\bar{S}^2$ is the mean square rate of strain ($=\bar{S}_{ij}\bar{S}_{ij}$). Finally, K_{SGS} solved for by substituting the scaling relation for ε_{KE} (eq. 14) into the SGS kinetic energy balance (eq. 15), or

$$K_{SGS} = \frac{(c_s\,\Delta)^2}{2^{1/2}} \left(\bar{S}^2 - \frac{2g}{Pr_t} \frac{\partial \bar{T}}{\partial x_3} \right)^{1/2} \qquad \bar{S}^2 > \frac{2g}{Pr_t} \frac{\partial \bar{T}}{\partial x_3} \tag{16}$$

The SGS eddy viscosity is set to zero if $\bar{S}^2$ is less than $2g/Pr_t \partial\bar{T}/\partial x_3$. However, this SGS "critical Richardson number" condition did not occur during our simulations. Further, the inclusion of SGS buoyancy production did not significantly affect the resulting values of K_{SGS} (Siegel, 1988) consistent with the assumption that Δ lies within the inertial subrange of turbulence.

The choices of values for c_s and Pr_t were made primarily by comparing simulated GS spectral energy distributions with theoretical Kolmogorov spectra for high Reynolds number turbulence, although a thorough literature survey was also made. The best results from this comparison are shown in figure 1. Six numerical experiments were performed to examine the degree of correspondence between the LES determined and theoretical radial wavenumber spectra and its relationship with variations in the values of c_s and Pr_t (Siegel, 1988). The final values of $c_s = 0.15$ and $Pr_t = 1.0$ best represented the theoretical spectra, especially for the temperature variance spectra (fig. 1). However, the LES KE spectra underestimate the Kolmogorov spectra by a factor of roughly five and exhibit a sharp "roll-up" as the GS cutoff wavenumber is approached (k_c=31). This "roll-up" indicates that the Smagorinsky SGS eddy viscosity is not adequately transferring KE across the GS cutoff and that there KE is "piling-up".

Spectral distributions of the magnitude of K_{SGS}, as well as the energy transfers due to the parameterized SGS fluxes, were also examined (Siegel and Domaradzki, 1991b). A "cartooned" representation of the spectral distribution of K_{SGS} (normalized by $(E(k_c)/k_c)^{1/2}$; where $E(k_c)$ is the value of the KE spectrum at the cutoff wavenumber, k_c) is shown in figure 2. The normalized K_{SGS} is to first order spectrally uniform, isotropically distributed and invariant in time. Similarly, SGS spectral energy transfers are white, indicating a uniform loss of energy at all scales. These results suggest that the Smagorinsky SGS eddy viscosity may be replaced by an isotropic, spectral SGS parameterization that scales as $(E(k_c)/k_c)^{1/2}$. A detailed analysis of the Smagorinsky SGS eddy viscosity and its energy transfers is presented in Siegel and Domaradzki (1991b).

THE CHOLLET AND LESIEUR (1981) SPECTRAL EDDY VISCOSITY

The Chollet and Lesieur (1981; CL81) spectral eddy viscosity has been derived using the Eddy Damped Quasi-Normal Markovian (EDQNM) turbulence closure theory calculation of the energy transfers across the GS cutoff (Chollet and Lesieur, 1981; Chollet, 1984; Lesieur, 1987). SGS eddy viscosities derived from alternative spectral closure formulations (Kraichnan, 1976), as well as from the results of direct isotropic turbulence simulations (Domaradzki *et al.*, 1987), are similar. The CL81

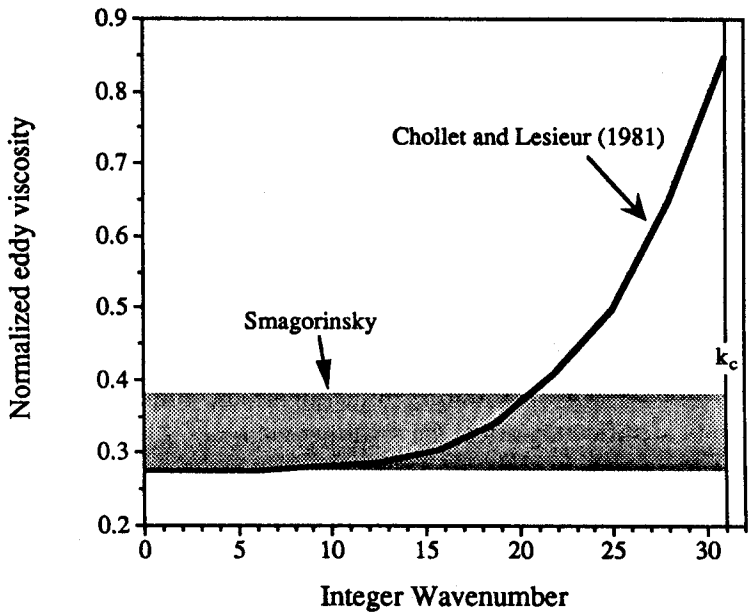

Figure 2: Spectral distribution of the CL81 eddy viscosity (Chollet and Lesieur, 1981) and the spectral distribution of the Smagorinsky SGS eddy viscosity calculated from the decaying simulations of stratified turbulence (based upon data from Siegel and Domaradzki, 1991b).

eddy viscosity has been used by Lesieur and his collaborators for examining stably-stratified turbulence (Métais, 1985; Lesieur, 1987; Lesieur *et al.*, 1988).

The CL81 eddy viscosity, $\nu_e(k)$, is formulated by the EDQNM evaluation of the spectral energy transfer across the GS cutoff (Δ) due to triad interactions which are both local (due to wavenumbers near the cutoff wavenumber, k_c) and nonlocal (from spectrally distant wavenumbers). The form of the CL81 spectral eddy viscosity (normalized by $(E(k_c)/k_c)^{1/2}$) is shown in figure 2. For low radial wavenumbers ($k<10$), the normalized CL81 eddy viscosity is equal to ~0.28 while it increases rapidly as the GS cutoff wavenumber is approached. This high wavenumber spectral cusp indicates the importance of local interactions to the spectral transfer of energy across the GS cutoff.

The CL81 SGS eddy viscosity is applied in spectral space where the term in (12) containing K_{SGS} is replaced with the CL81 spectral eddy viscosity ($\nu_e(k)$),

$$\frac{\partial}{\partial x_j}\left(K_{SGS}\,\bar{S}_{ij}\right) \quad \Rightarrow \quad -\nu_e(k)\,k^2\,\bar{u}_i \tag{17}$$

where $\nu_e(k)$ is equal to the normalized SGS eddy viscosity shown in figure 2 multiplied by the scaling factor, $((E(k_c)/k_c)^{1/2})$. A similar transformation is made for the heat equation. The CL81 spectral eddy viscosity ($\nu_e(k)$) and diffusivity ($\kappa_e(k)$) are related by a constant SGS Prandtl number (Pr_t=0.6; Chollet, 1984). Note that the normalized value of the Smagorinsky SGS eddy viscosity spectra, although uniform, is greater than the normalized CL81 viscosity at low wavenumbers and less at higher wavenumbers (fig. 2). In a sense, the Smagorinsky SGS eddy viscosity accounts only for the

nonlocal turbulent interactions represented by the low wavenumber plateau region of the CL81 SGS viscosity, but at a level higher than the CL81 plateau to account for its inefficiency of local energy transfers (Lesieur, 1987; Siegel and Domaradzki, 1991b).

The GS KE spectra calculated using the CL81 eddy viscosity are quantitatively similar to the theoretical Kolmogorov energy spectra (fig. 1) for the higher simulated wavenumbers (k>10). This subjective measure of SGS parameterization performance indicates that the CL81 eddy viscosity clearly outperforms the Smagorinsky SGS eddy viscosity. Another indication is the lack of a "roll-up" in the CL81 energy spectra near the cutoff wavenumber, indicating that the CL81 cusp is effective at removing energy near k_c. In addition to an increase in performance, the use of the CL81 eddy viscosity represents a substantial improvement in computational efficiency (about a factor of 2). This speedup comes from the fact that CL81 SGS parameterization does not require that $\partial(K_{SGS}\,\bar{S}_{ij})/\partial x_j$ be evaluated at each time step, which eliminates more than half of the 3-D fast Fourier transforms required to implement the Smagorinsky SGS parameterization.

LES EXPERIMENTS

We present the results of two LES experiments to investigate the dynamics and kinematics of oceanic internal gravity wave fields. The first experiment is the study of the decay of stably-stratified turbulence at oceanographically relevant length and time scales (Siegel, 1988; Siegel and Domaradzki, 1991a; 1991b). The initial wavenumber distribution is consistent with an extrapolation of the Garrett-Munk (GM) internal wave spectrum to scales smaller than 10 m. This experiment clearly shows many features of the so-called "turbulent collapse" (the transition from a fully turbulent flow to an internal wave dominated field). However, the present results illustrate several important differences from previous laboratory and *direct* numerical results. In particular, highly anisotropic, "pancake" structures are not formed coincident with the onset of the turbulent collapse. We speculate that these differences may be attributed to the extreme differences in Reynolds numbers for the two cases.

The second experiments are the preliminary investigations of the use of LES techniques to directly *determine eddy diffusivities for a steady GM ocean (Siegel, 1991).* Here, the lowest resolved wave modes are forced to maintain constant energy, consistent with GM amplitudes while the phases of the forced waves are determined dynamically. The long time integration (≥30 Nt) and steady forcing enables time/space mean values of the buoyancy flux and hence, the vertical eddy diffusivity (K_{BF}) to be directly determined. Values of vertical eddy diffusivity averaged over long time (≥20 Nt) and large space (125,000 m^3) scales are appropriate for use in oceanic circulation models. The direct K_{BF} determinations are compared with the results of several indirect turbulent energy dissipation rate methods (Osborn and Cox, 1972; Osborn, 1980). In addition, the dependency of K_{BF} upon N, the buoyancy frequency, is also investigated. These LES results are still preliminary as further experiments and detailed analyses are required. However, this successful "proof of concept" experiment suggests that LES techniques, when explicitly forced to *in situ* observations, may be a useful tool for examining mixing processes within the thermocline.

LES OF DECAYING OCEAN TURBULENCE

The first LES experiment to be discussed is the study of the decay of stratified turbulence at oceanographically relevant space and time scales. The temporal evolution and spatial structure of the decaying stratified turbulent flow are investigated where the initial conditions are represented by an extrapolation of the GM spectrum. These results will be addressed briefly here as they are discussed in detail in Siegel and Domaradzki (1991a) and (1991b).

The modeling domain (L) is chosen to be 10 m and the numerical resolution is 64^3. This results in a GS cutoff (Δ) equal to 15.6 cm. The choice of L (=10 m) was made to insure that the GS cutoff lies within the inertial subrange of turbulence. The separation between GS and SGS motions is done with an implicit boxcar filter and the Smagorinsky SGS eddy viscosity is used. Three simulations were made with buoyancy frequencies of 1, 3 and 10 cph and the equations of motion were integrated forward in time for 10 units of buoyancy time (Nt). Each experiment required 6.8 CPU hours of Cray XMP/48 time. For brevity, only the 1 cph case will be shown.

The initial conditions are based upon an extrapolation of the GM internal wave spectrum to scales less than 10 m. Of course the GM spectrum was not developed to correctly predict the variance at these scales. However, there does not exist a unified 3-D velocity and temperature finestructure spectrum that one could use to initialize the LES model, although several advances towards this goal have been made recently (e.g., Kunze *et al.*, 1990; M.C. Gregg, this volume). As it is recognized that the GM spectrum should not hold for scales less than 10 m, there is little reason to believe that the phases of the individual internal wave modes will follow linear theory either (e.g., Holloway, 1983; Müller *et al.*, 1986; Shen and Holloway, 1986). Hence, we randomized not only the internal wave mode phases, but the phase of each *component* of each wave mode. This will obviously result in an initial flow field that is highly unstable and its initial decay will be rapid and turbulent. The use of a fully random initial field is consistent with numerical turbulence procedures (e.g., Orszag and Patterson, 1972; Rogallo and Moin, 1984; Métais and Herring, 1989). Further details concerning the initialization procedure and its consequences may be found in Siegel and Domaradzki (1991a).

The temporal evolution of the domain averaged energetics and length scales is shown in figure 3. All of the component energy levels decay rapidly as expected. Rapid exchanges of vertical kinetic energy (VKE) and potential energy (PE) are observed during the decay's latter stages. These component energy exchanges are driven by internal gravity wave motions which give rise to a reversible buoyancy flux (BF). However, the internal waves cannot be linear as the domain-averaged BF is nonzero (Stewart, 1969). Evaluation of SGS energetics, fluxes and dissipation indicates that SGS processes regulated energy dissipation, but made negligibly small contributions to the total energetics and fluxes, consistent with the LES assumptions.

The evolution of the the Ozmidov (L_o) and the vertical integral (h) length scales provide additional insights into the state of decaying stratified turbulence. The Ozmidov scale is equal to

$$L_o = \left(\frac{\varepsilon}{N^3}\right)^{1/2} \tag{18a}$$

which represents the vertical scale where buoyancy and inertial forces equally influence the evolution of vertical momentum. That is, vertical scales larger than L_o will be affected by the stable

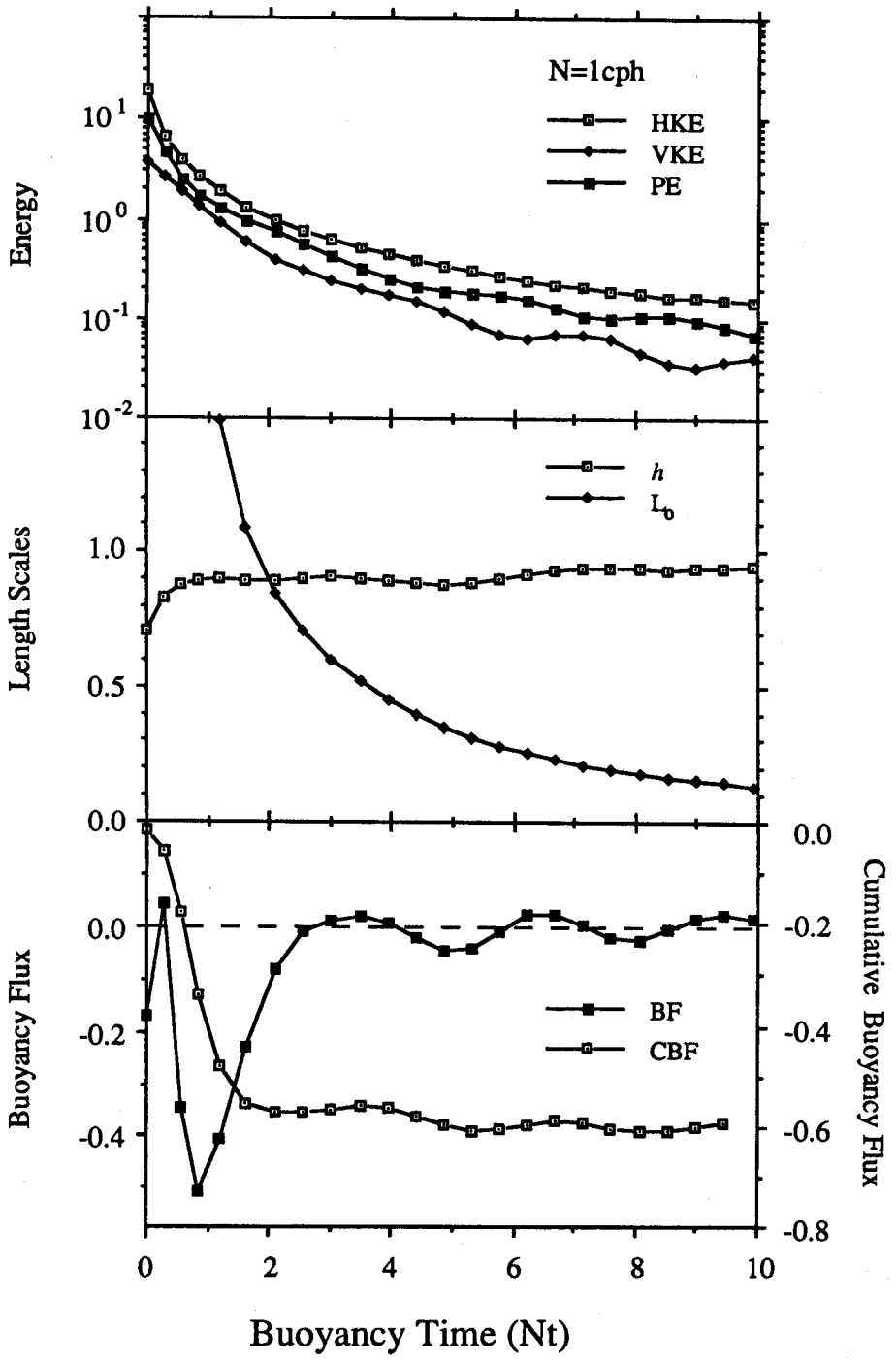

Figure 3: Temporal evolution of the domain averaged HKE, VKE and PE (upper panel), the vertical energy containing length scale, *h*, and the Ozmidov scale, L_o, (middle panel), and the buoyancy flux, BF, and cumulative buoyancy flux, CBF (lower panel). The mean stratification is 1 cph and the experiment is conducted for 10 buoyancy periods, Nt. ((from Siegel and Domaradzki, 1991a).

stratification. Whereas for scales smaller than L_o, these eddies will remain unaffected. Integral length scales are calculated by evaluating the most probable length scale from the kinetic energy spectra, or

$$h = \frac{\pi}{6}\left(\sum_{k_3=1}^{N/2} \hat{u}_i(k_3)\hat{u}_i(-k_3)/|k_3|\right)\left(\sum_{k_3=1}^{N/2} \hat{u}_i(k_3)\hat{u}_i(-k_3)\right)^{-1} \qquad (18b)$$

where $\hat{u}_i(k_j)$ here represents Fourier amplitudes of the i^{th} component of the velocity field in the j^{th} wavenumber direction and index summation is assumed. This definition for h is somewhat arbitrary as many other choices could have been made (Métais and Herring, 1989). It should be noted that h is related to the vertical extent of the kinetic energy structures and makes no distinction whether these structures are turbulent eddies or internal waves.

The vertical energy-containing scale (h) remains nearly constant while the Ozmidov scale (L_o) decreases rapidly with time (fig. 3). Initially, L_o is much larger than h indicating that the vertical motions of the energy-containing eddies are regulated primarily by inertial, or nonlinear, processes. However as L_o decreases, buoyancy forces become more important. This transition occurs at $Nt \cong 2$, indicating that the Froude number ($Fr \equiv (L_o/h)^{2/3}$) is equal to one. Note that this dynamical transition does not manifest itself in the evolution of h while synchronous oscillations in VKE and PE are most apparent after the transition. This behavior is also observed with different stratification intensities (Siegel and Domaradzki, 1991a).

Evidence of the turbulent collapse is most apparent in the temporal evolution of the buoyancy flux (BF; fig. 3). When BF is negative, VKE is converted to PE, effectively raising the fluid's center of mass. If this conversion happens irreversibly, the fluid's center of mass is permanently raised indicating that diapycnal mixing has occurred. A reversible BF shows up as internal wave motions. Irreversible aspects of BF are best illustrated by examining the cumulative buoyancy flux (CBF), or

$$CBF(t) = \int_0^t BF(\tau)\, d\tau \qquad (19)$$

which is shown in the bottom panel of figure 3. Early in its evolution ($Nt<2$), values of CBF decrease monotonically. After this period, CBF stops accumulating negative values and begins to oscillates in time. The transition from an irreversible accumulation of PE to reversible BF oscillations indicates that the initially turbulent flow evolves rapidly into a field of nonlinear internal waves.

The transition from a fully turbulent to a buoyancy dominated flow may be visualized by examining the temporal evolution of vertical slices of the absolute temperature ($\bar{T}(x;t) + T_s(z)$). An example of the temporal evolution in the absolute temperature is shown in figure 4 for Nt of 1, 2, 3 and 4. These spatial distributions give the appearance of a turbulent flow gradually evolving into an internal wave-dominated flow, with the general features described above. However, this transition does not appear to occur suddenly and these data cannot be used to visually determine the transition time. We have also analyzed 3-D topological structure of isotherm distributions which also provide useful visual evidence of the collapse (color plates may be found in Vasilopoulos, 1991).

The term "turbulent collapse" refers to the process of decay of stably-stratified, fully developed turbulence to a state where the vertical turbulent scales are suppressed by the background stratification (e.g., Dickey and Mellor, 1980; Stillinger *et al.*, 1982; Itsweire *et al.*, 1986; Lesieur, 1987; Hopfinger, 1987). This vertical scale suppression is thought to cause the initially 3-D eddies to

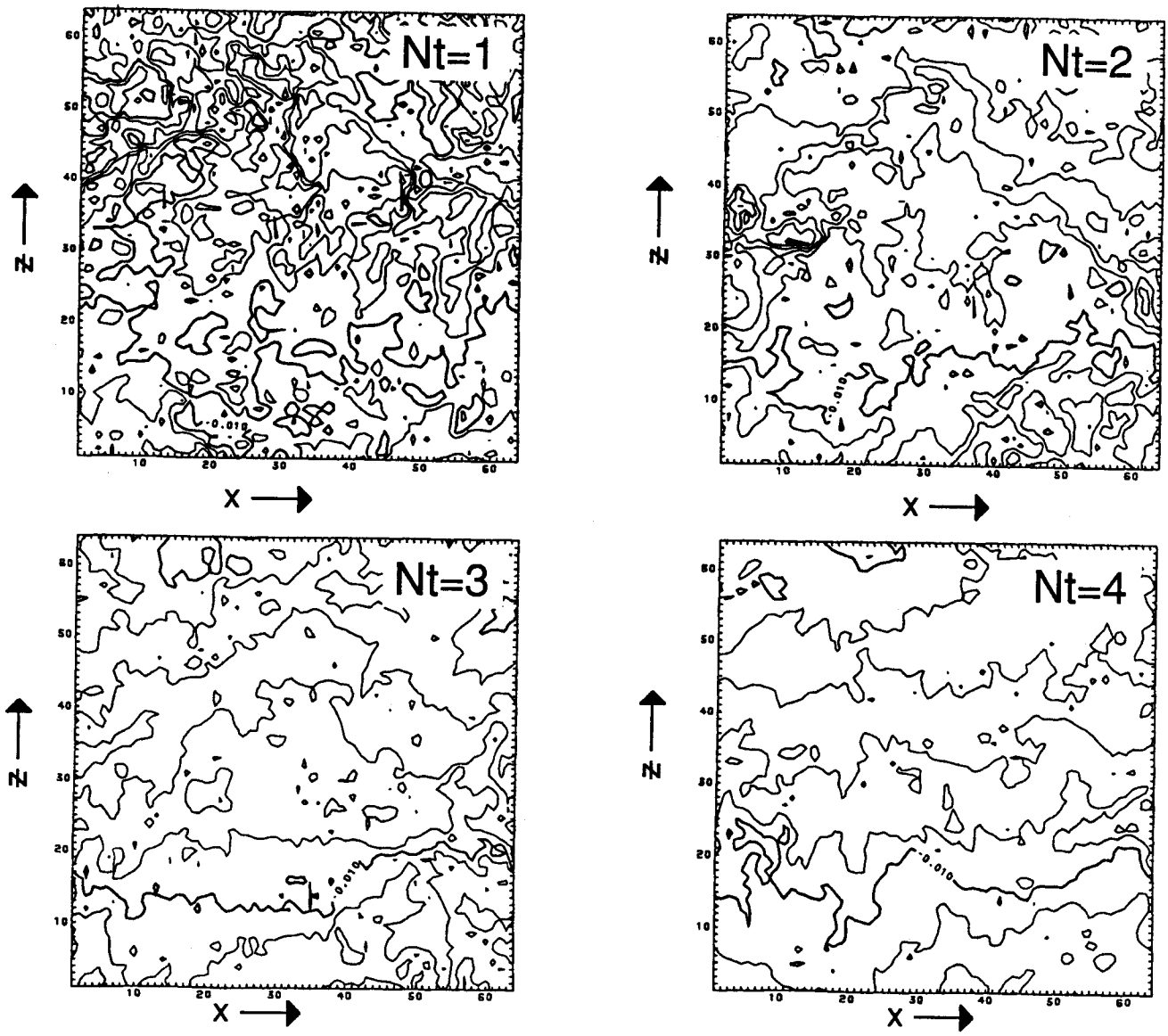

Figure 4: Temporal evolution of the vertical-horizontal sections of the absolute temperature ($T_s(z)$ + $\bar{T}(x,t)$) for buoyancy periods of 1, 2, 3, and 4. The mean stratification is 1 cph. (from Siegel and Domaradzki, 1991a).

"collapse" into nearly horizontal "pancake-like" vortices where their vertical scale is limited by L_o. Observations of these "pancake-like" eddies have been made primarily from laboratory flow visualizations (e.g., Lin and Pao, 1979; Hopfinger, 1987; Browand *et al.*, 1987), while reductions in energy decay rates and/or a vanishing buoyancy flux are often used as proxies of the collapse's occurrence (Dickey and Mellor, 1980; Stillinger *et al.*, 1982; Itsweire *et al.*, 1986; Hopfinger, 1987).

The LES results appear to give conflicting information about the occurrence of the turbulent collapse. For example, energy decay rates do not decrease significantly coincident with the onset of the turbulent collapse. Further, the size of the vertical integral scale (h) remains unaffected by the collapse, roughly

the same size as the horizontal energy-containing scale (l; not shown; Siegel and Domaradzki, 1991a). These results are unexpected as classical length scale phenomenology predicts that the vertical length scale of the *turbulent* eddies, and their KE, should decrease in a manner similar to the Ozmidov scale. Thus, we are not seeing a "pancaking" of the energy-containing eddies coincident with the collapse. However, the change in the nature of the BF indicates that the collapse has occurred (fig. 3).

The invariance of integral length scales implies that the dynamics of these energy-containing motions must have evolved from a turbulent state to one where buoyancy forces are important while retaining their size and isotropy. This lack of "pancaking" may be examined by addressing the evolution of the total vertical energy (TVE), the sum of VKE and PE. As the buoyancy flux acts only to exchange VKE and PE, BF will have absolutely no influence upon TVE. This means that vertical length scales characteristic of TVE will remain constant during the collapse. Similarly, the nonlinear energy cascades of TVE and hence, its energy decay rate will remain unaffected by the collapse. Thus, the onset of the collapse only indicates that the evolution of PE and VKE will be intertwined by a reversible BF and energy decay rates, as well as integral length scales, should remain unaffected by this dynamic transition This will remain true as long as molecular dissipation processes are *not* important for the evolution of the energy-containing motions ($Re_\lambda >> 1$).

Here, we suggest that this apparent lack of correspondence between the LES results and previous laboratory and *direct* numerical experiments is caused by extreme differences in the Reynolds numbers for the two cases. As described earlier, Reynolds numbers based upon Taylor length scales (Re_λ) corresponding to the oceanic internal wave field are $O(10^5)$ consistent with the LES results. However, laboratory or *direct* numerical experiments rarely give *initial* Re_λ values as great as 100. It should not be expected that these low Re_λ experiments can realistically simulate the interactions found within the oceanic internal wave field as molecular processes will have far too important roles in the evolution of the energy-containing eddies.

This Reynolds number dependency of the turbulent collapse is consistent with the results of a recent scaling analysis by Gargett (1988). Gargett's scaling indicates that for a high Reynolds number flow characteristic length scales will be isotropically distributed, whereas for a low Re_λ flow the vertical scales would be restricted. Her scaling holds only when the Froude number is O(1) and hence, only at the onset of the collapse. However, it is not clear whether the assumptions used in Gargett's scaling are valid (e.g., Van Atta, 1990; Yamazaki, 1990).

Unfortunately, we cannot state with certainty that this observed lack of "pancaking" is caused by the large LES-simulated Reynolds numbers. This is because there are many questions concerning the roles of the SGS method and the initial conditions upon the LES simulated flow field. One should note that the evolution of the buoyancy flux (a second order moment) is predicted consistent with the collapse onset while the spatial energy distributions (i.e., first order statistics) are clearly inconsistent with previous low-Re observations. It seems odd that the choice of the SGS parameterization, even an isotropic one like the Smagorinsky SGS eddy viscosity, would "correctly" predict the BF evolution, but not the flow energetics. Other SGS methods (CL81) which we have tried give nearly identical results. We believe that the reason for this is that the simulated high wavenumber motions are within the inertial subrange of turbulence and are locally isotropic (Siegel and Domaradzki, 1991b). This is consistent with the basic tenets of the large-eddy approximation described above. Therefore, the

application of an isotropic SGS eddy viscosity to parameterize the SGS energy fluxes in stratified turbulence may be appropriate.

Similarly, it seems unlikely that the initial conditions have much influence upon the final evolution of the flow field. We have initialized the LES experiments with a highly anisotropic energy distribution that rapidly becomes isotropic. As discussed above, this rapid reorganization of spectral energy is caused by the choice of random phases among wave components. Thus, it is unlikely that the initial anisotropic flow is controlling much of the flow's evolution. Further arguments supporting our conjecture of the importance of Reynolds numbers in the evolution of stratified turbulence is beyond the scope of this contribution. However, detailed experiments and analyses are required before the turbulent collapse can be considered to be an "understood" phenomena, particularly for high Reynolds number flows.

We suggest that the absence of "pancaking" in our LES results is due to the large simulated Reynolds numbers compared with previous laboratory and *direct* numerical experiments. If our LES results are truly representing the turbulent collapse, this suggests that the fundamental nature of decaying stably-stratified turbulence may be different at oceanographically relevant space and time scales compared with previous laboratory observations. This indicates that one should be cautious when applying low Reynolds number results to the oceanic internal wave field.

LES OF STEADY THERMOCLINE MOTIONS

Here, we illustrate preliminary results of a LES model of a steady GM ocean for directly determining values of the vertical eddy diffusivity. The quasi-steady forcing and long time integration enables values of the buoyancy flux (<BF>, where <•> represents a time-space average) and hence, values of the vertical eddy diffusivity (K_{BF}) to be calculated over long time scales ($\geq$ 20 Nt). The LES calculated K_{BF} values are determined over many hours and spatial scales of 50 m and are representative of vertical eddy diffusivities appropriate for use in oceanic general circulation models. Please note that these results are preliminary.

The GS equations of motion are numerically forced to maintain constant energy, consistent with GM spectral amplitudes, for the 8 wave modes where $|\mathbf{k}| = (1,1,1)$ (that is, for $\mathbf{k}=(1,1,1)$, $\mathbf{k}=(1,1,-1)$, $\mathbf{k}=(1,-1,1)$, etc.). The forcing amplitude is based upon the GM internal wave spectrum while the phases are determined by solving the equations of motion. This forcing method has been used in the numerical simulation of steady isotropic turbulence (Siggia and Patterson, 1978; Kerr, 1985). It has been shown that the nature of the forcing method (i.e., VKE to PE ratio, spectral weighting of the forcing function, etc.) can have significant impact on the simulated flow fields (e.g., Shen and Holloway, 1986; Holloway, 1988; Holloway and Ramsden, 1988). By selecting *a priori* the forcing wavenumber ($|\mathbf{k}| = (1,1,1)$), the ratio of VKE to PE (2/3) (and PE to HKE; 1/2) for the forced waves is fixed by the GM spectrum and is independent of the buoyancy frequency. Whether this choice of forcing is representative of the oceanic internal wave field, as well as its role in determining K_{BF}, is unknown at this time.

The domain is a triply periodic cube with dimensions of 50 m on a side. The numerical resolution is 96^3 resulting in a GS cutoff (Δ) of 52 cm. The Chollet and Lesieur (1981; CL81) spectral eddy viscosity is used to parameterize the SGS processes. Near-perfect correspondence is observed

between the theoretical Kolmogorov spectra and the LES calculated energy spectra suggesting that the CL81 SGS eddy viscosity is performing adequately (fig. 1). The flow field is initialized as in the decaying experiments and is numerically forced as described above. Three mean stratifications (1, 3 and 10 cph) are used and the GS equations of motion are integrated for 30 buoyancy periods (Nt). Statistical quantities (time/space means; $< \bullet >$) are calculated for the last 20 Nt of the simulations when the flow is nearly stationary. Statistical quantities are re-cast into dimensional units for ease in comparison with field observations. Each experiment requires about 12 CPU hours of Cray YMP 8/864 time (~20 CPU minutes per Nt).

Temporal evolution of the energetics and buoyancy flux are shown in figure 5 for the N = 3 cph experiment (the other experiments are qualitatively similar). A high degree of temporal reorganization is occurring while the energy levels are generally decreasing in time. This is due primarily to the energy variations of the zero wavenumber components, although there is some evidence of small changes in spectral energy levels after Nt = 10. As before with the decaying simulations, significant oscillations in VKE and PE are observed driven by a reversible buoyancy flux. However, the BF oscillations are not strictly periodic, indicating the existence of several internal wave modes.

Here, our goal is to use the results from the quasi-steady LES experiments to directly determine relevant mixing parameters. Space/time averages for kinetic and potential energy dissipation rates ($<\varepsilon_{KE}>$ and $<\varepsilon_{PE}>$) are given in Table 1. Values of $<\varepsilon_{KE}>$ range from 1.0×10^{-8} to 5.1×10^{-7} $m^2 s^{-3}$ consistent (although a bit high) with observed mean values (e.g., Gregg, 1987; 1989; Gregg and Sanford, 1988). The variation of the time/space mean values of $<\varepsilon_{KE}>$ and $<\varepsilon_{PE}>$ with buoyancy frequency, N, is shown in figure 6. Both $<\varepsilon_{KE}>$ and $<\varepsilon_{PE}>$ show a $N^{+7/4}$ dependency similar to the scaling results of Gargett and Holloway (1984) and the ε_{KE} parameterization of Gregg (1989). A direct comparison of the LES results with the Gregg's (1989) parameterization is presently underway. The ratio of $<\varepsilon_{PE}>$ to $<\varepsilon_{KE}>$ defines the mixing efficiency, η. Values of η are equal to 0.3 independent of N (Table 1), fairly consistent with *in situ* observations (e.g., Oakey, 1982).

Similarly, the vertical eddy diffusivity, K_{BF}, can be directly determined knowing the space/time averaged buoyancy flux, <BF>, or

$$K_{BF} \equiv - \frac{<BF>}{N^2} \qquad (20a)$$

The LES-calculated K_{BF} values all are positive indicating that on the average there is a down gradient flux of heat. Specifically, values of K_{BF} range from 6.0×10^{-6} to 6.7×10^{-4} $m^2 s^{-1}$ (Table 1) for the stratifications investigated and are generally consistent with the "abyssal recipes" value of 10^{-4} $m^2 s^{-1}$

TABLE 1: SPACE/TIME MEAN QUANTITIES FOR THE GM FORCED LES EXPERIMENTS

N (cph)	BF (m^2/s^3)	ε_{KE} (m^2/s^3)	ε_{PE}(m^2/s^3)	η	K_{BF} (m^2/s)	K_ε (m^2/s)	K_χ (m^2/s)
1	1.83×10^{-11}	1.01×10^{-8}	3.02×10^{-9}	0.30	6.01×10^{-6}	6.65×10^{-4}	9.93×10^{-4}
3	2.33×10^{-9}	5.77×10^{-8}	1.74×10^{-8}	0.30	8.48×10^{-5}	4.20×10^{-4}	6.35×10^{-4}
10	2.05×10^{-7}	5.11×10^{-7}	1.65×10^{-7}	0.32	6.73×10^{-4}	3.36×10^{-4}	5.43×10^{-4}

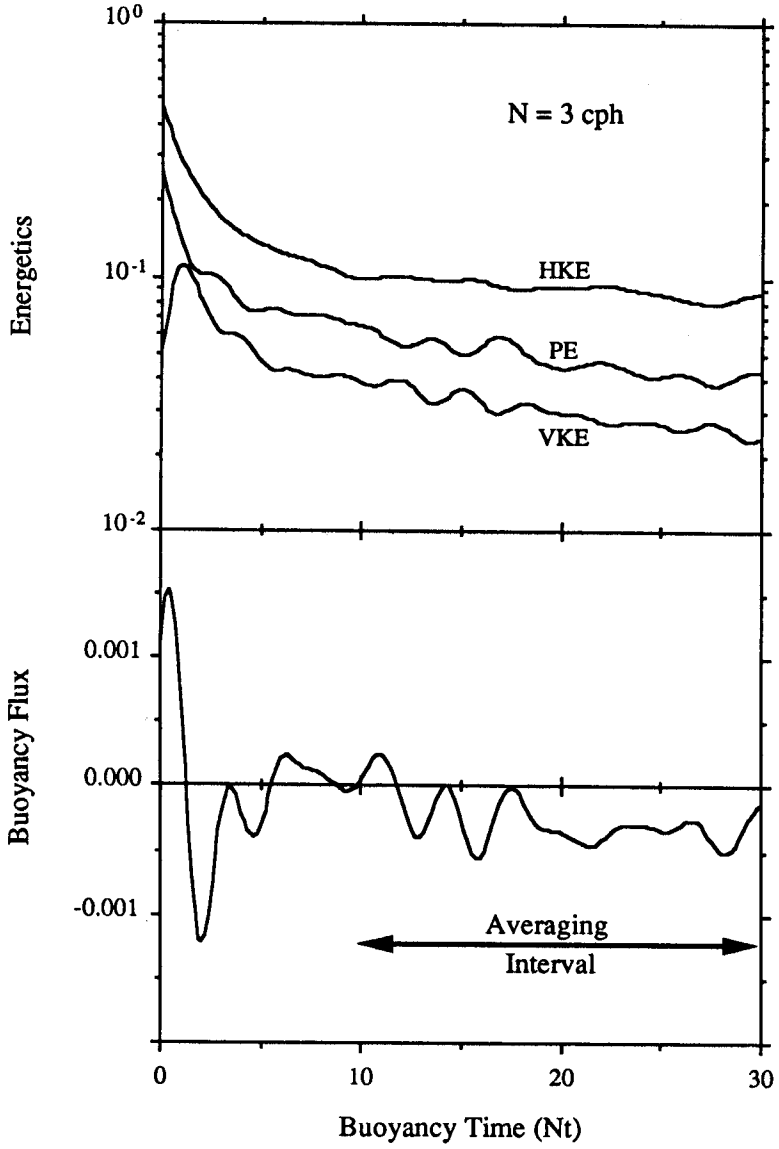

Figure 5: Temporal evolution of energetic quantities (HKE,VKE and PE), as well as the buoyancy flux (BF), for the forced GM LES experiment (N=3 cph). Averaging for the statistical calculations is made only for the last 20 Nt.

(Munk, 1966). However, values of K_{BF} increase dramatically with N (going as N^{+2}; fig. 7). At this point, we do not know exactly what is causing this anomalous dependency on N. However, it seems likely that the nature of the numerical forcing can have an undue influence upon K_{BF}. Indications of this are apparent when one compares the space/time averaged <BF> and $<\varepsilon_{PE}>$ for the N=10 cph experiment (Table 1). For this experiment, values of <BF> are greater than $<\varepsilon_{PE}>$ indicating that more energy is being transferred into PE from VKE than is being removed by diffusive processes. For a simplified "production (+ forcing) equals dissipation" PE budget to hold, there must be a mechanism to transfer this energy somewhere else. We think that the "culprit" may be the forcing mechanism

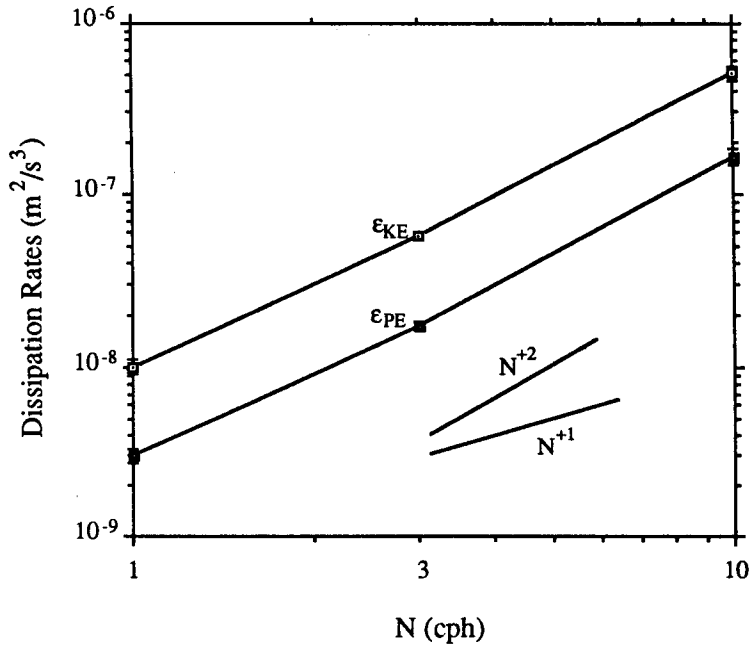

Figure 6: Dependency of space/time mean values of $\langle \varepsilon_{KE} \rangle$ and $\langle \varepsilon_{PE} \rangle$ upon buoyancy frequency, N. Standard deviations are shown by the error bars. Spectral slopes of N^{-1} and N^{-2} are shown.

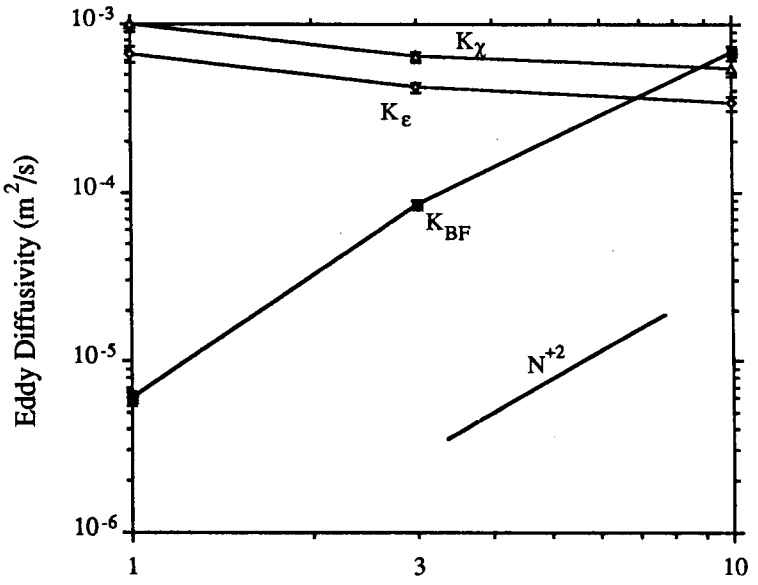

Figure 7: Dependency of space/time mean values of LES determined vertical eddy diffusivities (K_{BF}, K_ε and K_χ) upon buoyancy frequency, N. Standard deviations are shown as the error bars. A spectral slope of N^{+2} is also shown.

where PE is actually removed by the forcing. We are presently investigating this in detail. It should be mentioned that the time averaged BF will give the correct irreversible exchange of KE to PE (e.g., Lombard *et al.*, 1990) as it is not necessary to calculate the change in the background stratification in order to determine mixing coefficients (e.g., Winters and D'Asaro, 1990).

Several parameterization methods have been developed to predict values of vertical eddy diffusivity from measurements of turbulence dissipation rates. These indirect methods solve simplified turbulence variance budgets to determine values of vertical eddy diffusivity (e.g., Osborn and Cox,

1972; Osborn, 1980; Moum, 1990). For example, if the temperature variance dissipation rate, χ, is known, the temperature variance budget may be solved to give the eddy diffusion of heat, K_χ, (Osborn and Cox, 1972), or

$$K_\chi \equiv \frac{<\chi>}{(dT_s/dz)^2} \qquad (20b)$$

where dT_s/dz is the mean temperature gradient. Another method involves solving a simplified turbulent kinetic energy budget to provide an *upper* bound for values of the vertical eddy diffusivity (Osborn, 1980). After the ratio of shear to buoyancy production of turbulent kinetic energy is decided upon, values of ε_{KE} are used to provide the eddy diffusivity, K_ε, or

$$K_\varepsilon \equiv 0.2 \frac{<\varepsilon_{KE}>}{N^2} \qquad (20c)$$

In the past, eddy diffusivity parameterization assumptions have been tested by evaluating variance budgets, not by direct comparison to measurements of the buoyancy flux (Garrett, 1979; Washburn, 1987). Only recently have direct determinations of vertical velocity fluctuations enabled these comparisons to be made (Moum, 1990).

Values of K_χ and K_ε for the forced LES experiments range from 3.4×10^{-4} to 9.9×10^{-4} $m^2\ s^{-1}$ and hence, vary considerably less than the two-decade range of variation observed for K_{BF} (Table 1). Generally, K_χ and K_ε are both greater than the directly determined K_{BF}. This was also observed in the *in situ* K_{BF} determinations by Moum (1990). However, the dependencies of K_χ and K_ε on N are very different than the dependency observed for K_{BF} (going like $N^{-1/4}$ instead of N^{+2}; fig. 7).

Obviously, there is a discrepancy in the vertical eddy diffusivities predicted by the direct and the variance dissipation methods. These differences are particularly apparent in the dependency of the estimated eddy diffusivities on the background stratification intensity, N. As discussed previously, the interactions of the numerical forcings with the determination of the BF are not well understood. However, the fact that the indirect methods do such a poor job in predicting K_{BF}, regardless of the what's forcing the large-scale (50 m) internal waves, indicates that these indirect methods are not adequately parameterize vertical eddy diffusivities for the conditions numerically simulated.

The existence of domain averaged BF oscillations in the present numerically forced LES experiments may have some interesting observational consequences. That is, although the domain-averaged BF is calculated over a volume equal to 125,000 m^3, its value is **not** stationary (fig. 5). Thus, instantaneous determinations of the buoyancy flux, even when averaged over a large spatial scales, may not adequately provide the necessary data to determine vertical eddy diffusivities for use in general circulation models. These large-scale ocean models require that small-scale internal wave "noise" be filtered out in terms of an effective eddy diffusivity. The present observations suggest that long time and large space integrations or *in situ* observations are necessary before relevant eddy diffusivities are to be determined.

WHAT'S NEXT?

The GM forced LES experiments have successfully replicated many of the dynamical quantities characteristic of the ocean's internal wave field. Specifically, direct calculations of vertical eddy

diffusivity, turbulent dissipation rates, and mixing efficiency have been surprisingly well in line with oceanographic thinking. Frankly, the fact that the *sign* of the eddy diffusivity was correct was a cause for celebration in Santa Barbara!! However, the anomalous dependency of K_{BF} on N raises doubts that our LES model is *realistically* simulating the internal wave field. Of course, there are many possibilities. The details of the numerical forcing, the omission of planetary vorticity (and hence, near-inertial waves), the restricted spatial scales simulated (< 50 m), the triply-periodic boundary conditions, possible lack of stationarity, as well as the subgrid scale parameterization method all could have contributed to the anomalous dependency of K_{BF} on N. Presently, we think that the "culprit" is the forcing mechanism and we are investigating, in detail, the energy transfers at the forcing wavenumber. This is not to say that each of the possibilities listed above do not need to be improved upon. In order for LES techniques to be of any use to oceanographers, the assumptions and mechanisms used to produce the simulations *must* be continually tested and evaluated.

We are presently implementing planetary vorticity (the f-plane approximation) into our LES model. This in the view of many is a serious omission in producing realistic simulations of the internal wave field. The inclusion of planetary vorticity (f-plane approximation) will enable us to force a LES with prescribed near-inertial waves. *In situ* observations have shown that much of the velocity finestructure is associated with near-inertial waves (Kunze *et al.*, 1990) and that these near-inertial waves can give rise to patches of turbulence (Gregg *et al.*, 1986). This improvement in the realism of the forcing mechanism should only help the LES model better replicate the internal wave field. An interesting hypothesis is that dependency of ε_{KE} on N, or for that matter K_{BF} on N, may depend upon the nature of how energy is fed into the internal wave field.

Eventually, it is envisioned that LES models can be used with *in situ* observations to provide "data" of the internal wave field that are presently unobtainable. Such a coupling would enable eddy diffusivities to be estimated for specific field experiments. This approach is similar to how hydrographic inverse or regional circulation models are used to give information about fluxes, vorticity and energy transfers that are, at best, difficult to determine from the field observations alone. Thus, the combination of field and numerical approaches may prove to be highly synergistic, allowing many new questions concerning the ocean's internal wave field to be addressed.

ACKNOWLEDGMENTS - The author would like to thank Peter Müller for inviting him to the 1991 'Aha Huliko'a Winter Workshop. Comments on this manuscript by Libe Washburn, Sally MacIntyre and Andrzej Domaradzki were extremely helpful. As always, the support, encouragement and guidance of Andrzej Domaradzki and Tommy Dickey is gratefully appreciated. Programming assistance from Ms. Xiaoning Duan has been instrumental in the success of the forced GM experiments which have been supported by the Office of Naval Research (N00014-90-J-1914). Supercomputer time has been provided by grants from the San Diego Supercomputer Center which is supported by the National Science Foundation.

REFERENCES

Browand, F.K., D. Guyomar, and S.-C. Yoon, 1987: The behavior of a turbulent front in a stratified fluid: experiments with an oscillating grid. *J. Geophys. Res.*, **92**, 5329-5341.

Canuto, C., M.Y. Hussaini, A. Quarteroni, and T.A. Zang, 1988: *Spectral Methods in Fluid Dynamics*. Springer-Verlag, p 567.

Chollet, J.P., and M. Lesieur, 1981: Parameterization of small scales of three-dimensional isotropic turbulence utilizing spectral closures. *J. Atmos. Sci.*, **38**, 2747-2757.

Chollet, J.P., 1984: Two point closures as a subgrid scale modeling for large eddy simulations. In: *Turbulent Shear Flows IV*, F. Durst and B. Launder (eds.), 62-72.

Clark, R.A., J.H. Ferziger and W.C. Reynolds, 1979: Evaluation of subgrid-scale turbulence models using a fully simulated turbulent flow. *J. Fluid Mech.*, **91**, 1-16.

Deardorff, J.W., 1970: A numerical study of three-dimensional turbulent channel flow at large Reynolds numbers. *J. Fluid Mech.*, **41**, 453-480.

Deardorff, J.W., 1973: Three-dimensional numerical modeling of the planetary boundary layer. *Workshop on Micrometeorology*, D. Haugen, ed., American Meteorological Society, 271-311.

Deardorff, J.W., 1980: Stratocumulus-capped mixed layer derived from a three-dimensional model. *Bound.-Layer Meteor.*, **18**, 495-527.

Dickey, T.D., and G.L. Mellor, 1980: Decaying turbulence in neutral and stratified fluids. *J. Fluid Mech.*, **99**, 13-31.

Domaradzki, J.A., R.W. Metcalfe, R.S. Rogallo and J.J. Riley, 1987: Analysis of subgrid-scale eddy viscosity with use of results from direct numerical simulations. *Phys. Rev. Lett.*, **58**, 547-550.

Ebert, E.E., U. Schumann and R.B. Stull, 1989: Nonlocal turbulence mixing in the convective boundary layer. *J. Atmos. Sci.*, **46**, 2178-2207.

Eidson, T.M., 1985: Numerical simulation of the turbulent Rayleigh-Bénard problem using subgrid modelling. *J. Fluid Mech.*, **158**, 245-268.

Ferziger, J.H., 1983: Higher-level simulations of turbulent flows. In: *Computational Methods for Turbulent, Transonic, and Viscous Flows*. J.A. Essers (ed.), 93-182, Hemisphere Pub., Washington, D.C.

Gallacher, P.C., 1990: Large-eddy simulations of the turbulent boundary layer in the upper ocean. *Trans. Amer. Geophys. Union, EOS*, **71**, 1354 (abstract only).

Gargett, A.E., 1988: The scaling of turbulence in the presence of stable stratification. *J. Geophys. Res.*, **93**, 5021-5036.

Gargett, A.E., and G. Holloway, 1984: Dissipation and diffusion by internal wave breaking. *J. Mar. Res.*, **42**, 15-27.

Gargett, A.E., P.J. Hendricks, T.B. Sanford, T.R. Osborn, and A.J. Williams III, 1981: A composite spectrum of vertical shear in the upper ocean. *J. Phys. Oceanogr.*, **11**, 1258-1271.

Gargett, A.E., T.R. Osborn, and P.W. Nasmyth, 1984: Local isotropy and the decay of turbulence in a stratified fluid. *J. Fluid Mech.*, **144**, 231-280.

Garrett, C.J.R., 1979: Mixing in the ocean interior. *Dyn. Atmos Oceans*, **3**, 239-265.

Garrett, C., and W. Munk, 1972: Space-time scales of internal waves. *Geophys. Fluid Dyn.*, **2**, 225-264.

Garrett, C., and W. Munk, 1975: Space-time scales of internal waves: A progress report. *J. Geophys. Res.*, **80**, 291-297. (also, corrigendum *J. Geophys. Res.*, **80**, 3924)

Gregg, M.C., 1987: Diapycnal mixing in the thermocline: A review. *J. Geophys. Res.*, **92**, 5249-5286.

Gregg, M.C., 1989: Scaling turbulent dissipation in the thermocline. *J. Geophys. Res.*, **94**, 9686-9698.

Gregg, M.C., and T.B. Sanford, 1988: The dependence of turbulent dissipation on stratification in a diffusively stable thermocline. *J. Geophys. Res.*, **93**, 12,381-12,392.

Gregg, M.C., E.A. D'Asaro, T.J. Shay, and N. Larson, 1986: Observations of persistent mixing and near-inertial waves internal waves. *J. Phys. Oceanogr.*, **16**, 856-885.

Holland, W.R. and L.B. Lin, 1975: On the origin of mesoscale eddies and their contribution to the general circulation of the ocean. I. A preliminary numerical experiment. *J. Phys. Oceanogr.*, **5**, 642-657.

Holloway, G., 1983: A conjecture relating oceanic internal waves and small-scale processes. *Atmos.-Ocean*, **21**, 107-122.

Holloway, G., 1988: The buoyancy flux from internal gravity wave breaking. *Dyn. Atmos. Oceans*, **12**, 107-125.

Holloway, G., and D. Ramsden, 1988, Theories of internal wave interaction and stably-stratified turbulence: Testing against direct numerical experimentation. In: *Small-Scale Turbulence and Mixing in the Ocean*, J.C.J. Nihoul and B.M. Jamart (eds.), 363-377, Elsevier, New York.

Hopfinger, E.J., 1987: Turbulence in stratified fluids: A review. *J. Geophys. Res.*, **92**, 5287-5303.

Itsweire, E.C., K.N. Helland, and C.W. Van Atta, 1986: The evolution of grid-generated turbulence in a stably stratified fluid. *J. Fluid Mech.*, **162**, 299-338.

Kerr, R.M., 1985: Higher-order derivative correlations and the alignment of small-scale structures in isotropic numerical turbulence. *J. Fluid Mech.*, **153**, 31-58.

Kraichnan, R.H., 1976: Eddy viscosity in two and three dimensions. *J. Atmos. Sci.*, **33**, 1521-1536.

Kunze, E., M.G. Briscoe and A.J. Williams III, 1990: Interpreting shear and strain fine structure from a neutrally buoyant float. *J. Geophys. Res.*, **95**, 18,111-18,125.

Ledwell, J.R., and A.J. Watson, 1991: The Santa Monica Basin tracer experiment: A study of diapycnal and isopycnal mixing. In press: *J. Geophys. Res.*

Leonard, A., 1974: Energy cascades in large eddy simulations of turbulent fluid flows. *Advances in Geophysics*, Vol. 18, Academic Press, 237-248.

Lesieur, M., 1987: *Turbulence in Fluids*. Martius Nijhoff Publ., Dordrecht, The Netherlands, p 286.

Lesieur, M., and R. Rogallo, 1989: Large-eddy simulation of passive scalar diffusion in isotropic turbulence. *Phys. Fluids A*, **1**, 718-722.

Lesieur, M., O. Métais, and H. Laroche, 1988: Numerical simulations of turbulent stably-stratified and free shear flows. (extended abstract), 57-60, In: *Eighth Symposium on Turbulence and Diffusion*, American Meteorological Society, Boston MA.

Lienhard V, J.H, and C.W. Van Atta, 1990: The decay of thermally stratified turbulence. *J. Fluid Mech.*, **210**, 57-112.

Lin, J.T., and Y.H. Pao, 1979: Wakes in stratified fluids. *Ann. Rev. Fluid Mech.*, **11**, 317-338.

Lombard, P.N., D.D. Stretch, and J.J. Riley, 1990: Energetics of a stably stratified mixing layer. *Proc. 9th Symp. Turb. Diff.*, 202-205.

Mansour, N.N., P. Moin, W.C. Reynolds, and J.H. Fertziger, 1979: Improved methods for large eddy simulations of turbulence. In: *Turbulent Shear Flows I*, F. Durst, B. Launder, F. Schmidt, and J. Whitelaw (eds.), Springer-Verlag, 386-401.

Mason, P.J., and S.H. Derbyshire, 1990: Large-eddy simulation of the stably-stratified atmospheric boundary layer. *Bound.-Layer Met.*, **53**, 117-162.

McWilliams, J.C., P.C. Gallacher, C.-H. Moeng, and J. Wyngaard, 1990: Large-eddy simulations of oceanic boundary layers. Presented at the International Workshop on Large Eddy Simulation, St. Petersburg, FL, December, 1990.

Métais, O., 1985: Evolution of three dimensional turbulence under stratification. In: Lesieur, M., 1987: *Turbulence in Fluids.* (also presented at Turbulent Shear Flows VI).

Métais, O., and J.R. Herring, 1989: Numerical simulations of freely evolving turbulence in stably stratified fluids. *J. Fluid Mech.*, **202**, 117-148.

Moeng, C.-H., 1984: A large-eddy simulation model for the study of planetary boundary-layer turbulence. *J. Atmos. Sci.*, **41**, 2052-2062.

Moeng, C.-H. and J.C. Wyngaard, 1988: Spectral analysis of large-eddy simulations of the convective boundary-layer. *J. Atmos. Sci.*, **45**, 3573-3587.

Moum, J. N., 1990: The quest for Kρ - Preliminary results from direct measurement of turbulent fluxes in the ocean. *J. Phys. Oceanogr.*, **20**, 1980-1984.

Müller, P., 1988: Vortical Motions. In: *Small-Scale Turbulence and Mixing in the Ocean,* J.C.J. Nihoul and B.M. Jamart (eds.), 285-301, Elsevier, New York.

Müller, P., G. Holloway, F. Henyey, and N. Pomphrey, 1986: Nonlinear interactions among internal gravity waves. *Rev. Geophys.*, **24**, 493-536.

Munk, W.H., 1966: Abyssal recipes. *Deep-Sea Res.*, **13**, 707-730.

Munk, W., 1981: Internal waves and small-scale processes. In: *Evolution of Physical Oceanography,* B. Warren and C. Wunsch (eds.), The MIT Press, Cambridge, MA, 264-291.

Oakey, N.S., 1982: Determination of the rate of dissipation of turbulent energy from simultaneous temperature and velocity shear microstructure measurements. *J. Phys. Oceanogr.*, **12**, 256-271.

Orszag, S., 1971: Numerical simulation of incompressible flows within simple boundaries: Accuracy. *J. Fluid Mech.*, **49**, 75-112.

Orszag, S., and G.S. Patterson, 1972: Numerical simulation of three-dimensional homogeneous isotropic turbulence. *Phys. Rev. Lett.*, **28**, 76-79.

Osborn, T.R., 1980: Estimates of the local rate of vertical diffusion from dissipation measurements. *J. Phys. Oceanogr.*, **10**, 83-89.

Osborn, T.R., and C.S. Cox, 1972: Oceanic fine structure. *Geophys. Fluid Dyn.*, **3**, 321-345.

Piomelli, U., P. Moin, and J.H. Ferziger, 1989: Model consistency in large-eddy simulation of turbulent channel flows. *Phys. Fluids*, **31**, 1884-1891.

Ramsden, D. and G. Holloway, 1991: Vortex-wave interactions in stably stratified turbulence. Submitted to *J. Geophys. Res.*

Riley, J.J., R.W. Metcalfe, and M.A. Weissman, 1981: Direct numerical simulations of homogeneous turbulence in density-stratified fluids. *AIP Conf. Nonlinear Properties of Internal Waves.* B. West (ed.), 79-112.

Rogallo, R., and P. Moin, 1984: Numerical simulations of turbulent flows. *Ann. Rev. Fluid Mech.*, **16**, 99-137.

Schmidt, H., and U. Schumann, 1989: Coherent structure of the convective boundary layer derived from large-eddy simulations. *J. Fluid Mech.*, **200**, 511-562.

Schumann, U., 1975: Subgrid-scale model for finite difference simulations of turbulent shear flows in plane channels and annuli. *J. Comp. Phys.*, **18**, 376-404.

Schumann, U., 1991: Subgrid length-scales for large-eddy simulation of stratified turbulence. In: *Theoretical and Computational Fluid Dynamics*, T. Gatski and C. Speziale (eds.), Springer-Verlag, Berlin.

Shen, C.Y., and G. Holloway, 1986: A numerical study of the frequency and the energetics of nonlinear internal gravity waves. *J. Geophys. Res.*, **91**, 953-973.

Siegel, D.A., 1988: Large-eddy simulation of the decay of a small-scale oceanic internal gravity wave field, Ph.D. Dissertation, Department of Geological Sciences, University of Southern California, p 187.

Siegel, D.A., 1991: Large-eddy simulation of steady thermocline motions. In preparation.

Siegel, D.A., and J.A. Domaradzki, 1991a: Large-eddy simulation of the decay of stably-stratified oceanic turbulence, I: Model development and observations of temporal variability. Submitted to *J. Phys. Oceanogr.*

Siegel, D.A., and J.A. Domaradzki, 1991b: Large-eddy simulation of the decay of stably-stratified oceanic turbulence, II: Characterization of the kinematic and dynamic structure. Submitted to *J. Phys. Oceanogr.*

Siegel, D.A., and A.J. Plueddemann, 1991: The motion of a solid sphere in an oscillating flow: An evaluation of remotely-sensed Doppler velocity estimates in the sea. *J. Atmos. Oceanic Tech.*, **8**, 296-304.

Siggia, E.D., and G.S. Patterson, 1978: Intermittency effects in a numerical simulation of stationary three-dimensional turbulence. *J. Fluid Mech.*, **86**, 567-592.

Smagorinsky, J., 1963: General circulation experiments with the primitive equations. *Mon. Wea. Rev.*, **91**, 99-164.

Smagorinsky, J., 1990: Some historical remarks on the use of non-linear eddy viscosities in geophysical models. Presented at the International Workshop on Large Eddy Simulation, St. Petersburg, FL, December, 1990.

Stewart, R.W., 1969: Turbulence and waves in a stratified atmosphere. *Radio Sci.*, **4**, 1269-1278.

Stillinger, D.C., K.N. Helland, and C.W. Van Atta, 1983: Experiments on the transition of homogeneous turbulence to internal waves in a stratified fluid. *J. Fluid Mech.*, **131**, 91-122.

Tennekes, H., and J.L. Lumley, 1972: *A First Course in Turbulence*, The MIT Press, Cambridge, MA., p 300.

Van Atta, C., 1990: Comment on "The scaling of turbulence in the presence of stable stratification" by A.E. Gargett. *J. Geophys. Res.*, **95**, 11,673-11,674.

Vasilopoulos, A., 1991: Volume imaging: A new world view. *Comp. Graphics World*, April, 63-72.

Washburn, L., 1987: Two-dimensional observations of temperature microstructure in a coastal region. *J. Geophys. Res.*, **92**, 10,787-10,798.

Winters, K.B., and E.A. D'Asaro, 1990, Diapycnal mixing associated with a wave breaking event. *Trans. Amer. Geophys. Union, EOS*, **71**, 1360 (abstract).

Wyngaard, J. (ed.), 1984: *Large-Eddy Simulation: Guidelines for its Application to Planetary Boundary Layer Research.* Report from the Working Group on Large Eddy Simulation, Boulder, CO., p 122.

Yakhot, A., S.A. Orszag, V. Yakhot, and M. Israeli, 1989: Renormalization group formulation of large-eddy simulations. *J. Sci. Comp.*, **4**, 139-158.

Yamazaki, H., 1990: Stratified turbulence near a critical dissipation rate. *J. Phys. Oceanogr.*, **20**, 1583-1598.

Yoshizawa, A., 1982: A statistically derived subgrid scale model for large eddy simulation of turbulence. *Phys. Fluids*, **25**, 1532-1538.